

South Dakota State University

Open PRAIRIE: Open Public Research Access Institutional Repository and Information Exchange

Electronic Theses and Dissertations

2018

Optimization of Microfluidic Particle Separator Geometry Using Computational Fluid Dynamics

Joseph Petersen

South Dakota State University

Follow this and additional works at: <https://openprairie.sdstate.edu/etd>



Part of the [Dynamics and Dynamical Systems Commons](#), and the [Mechanical Engineering Commons](#)

Recommended Citation

Petersen, Joseph, "Optimization of Microfluidic Particle Separator Geometry Using Computational Fluid Dynamics" (2018). *Electronic Theses and Dissertations*. 2419.

<https://openprairie.sdstate.edu/etd/2419>

This Thesis - Open Access is brought to you for free and open access by Open PRAIRIE: Open Public Research Access Institutional Repository and Information Exchange. It has been accepted for inclusion in Electronic Theses and Dissertations by an authorized administrator of Open PRAIRIE: Open Public Research Access Institutional Repository and Information Exchange. For more information, please contact michael.biondo@sdstate.edu.

OPTIMIZATION OF MICROFLUIDIC PARTICLE SEPARATOR GEOMETRY USING
COMPUTATIONAL FLUID DYNAMICS

BY

JOSEPH PETERSEN

A thesis submitted in partial fulfilment of the requirements for the

Master of Science

Major in Mechanical Engineering

South Dakota State University

2018

OPTIMIZATION OF MICROFLUIDIC PARTICLE SEPARATOR GEOMETRY USING
COMPUTATIONAL FLUID DYNAMICS

This dissertation is approved as a creditable and independent investigation by a candidate for the Master of Science in Mechanical Engineering degree and is acceptable for meeting the dissertation requirements for this degree. Acceptance of this does not imply that the conclusions reached by the candidates are necessarily the conclusions of the major department.

Jeffrey Doorn, Ph.D.
Dissertation Advisor

Date

Kurt Basset, Ph.D.
Head, Department of Mechanical Engineering

Date

Kirchell Doerner
Dean, Graduate School

Date

I dedicate this work to my family and friends that made the college experience the most enjoyable time of my life.

ACKNOWLEDGEMENTS

I would like to acknowledge the generous support I received from my family and friends, my advisor Dr. Doom, who has been excellent to work for and always supportive, whether it be related to research work or help on homework, Dr. Yoon, for approaching Dr. Doom about this project, for teaching micro-fabrication techniques and the use of all the laboratory equipment used in the project, all my teachers and classmates that listened to presentations and gave valuable feedback, and Justin Pading for providing the original picture of blood cells under a microscope.

CONTENTS

ABBREVIATIONS	vii
LIST OF FIGURES	viii
LIST OF TABLES	ix
ABSTRACT	x
1 INTRODUCTION	1
1.1 DEFINITIONS	1
1.2 OVERVIEW	1
1.3 THESIS CONTRIBUTIONS	3
1.4 CELL SEPARATION AND ISOLATION	4
1.4.1 RARE CELL CAPTURE AND ISOLATION	4
1.4.2 CIRCULATING TUMOR CELLS	4
1.4.3 CELLSEARCH® CTC TEST SYSTEM	5
1.4.4 MICROFLUIDIC PLATFORMS FOR CTC ISOLATION	5
1.5 MICROFLUIDICS	5
1.6 COMPUTATIONAL FLUID DYNAMICS	9
1.6.1 THE NAVIER-STOKES EQUATIONS	10
1.6.2 DISCRETE ELEMENT METHOD	10
1.6.3 STAR-CCM+	13
2 METHOD	13
2.1 MESH	13
2.2 PHYSICS MODELS	15
2.3 MODEL DEVELOPMENT	16
2.4 PROOF OF CONCEPT MODEL	22

2.5	SINGLE DEM PARTICLE SIMULATION	25
2.6	DEVICE FABRICATION	25
3	RESULTS	26
3.1	SIMULATION RESULTS	26
3.2	EXPERIMENTAL RESULTS	29
4	INTERPRETATION	31
4.0.1	CAUSES OF DIFFERENCE BETWEEN SIMULATION AND EXPERIMENT	31
5	CONCLUSION	32
	REFERENCES	33

LIST OF FIGURES

1	Cells perform a variety of functions for living organisms. For example, blood cells in the human circulatory system transport nutrients across the body (left), while plant cells (right) provide a rigid structure for the organism in addition to other critical functions.	2
2	Cell is guided to trapping passage by hydrodynamic forces (1). Because the trapping passage is plugged, other cells are guided around the trapping passage thorough the longer serpentine passage to the next trap in the array (2). When trapping passages are full, cells are cultured (3). Cultured cells are then removed from device for study (4).	3
3	Cells in a tumor of human colon tissue at 400X magnification. Tumors of epithelial tissue have the potential to shed into the circulatory system and become CTCs.	5
4	The CELLSEARCH® System for identification, isolation, and enumeration of circulating tumor cells from a simple blood test.	6
5	Microfluidic devices scale down the processes of laboratory equipment to sub millimeter scale.	7
6	Computational fluid dynamics is used simulate and visualize the flow of fluid around objects, and in some cases can substitute for costly experimental tests.	9
7	DEM objects used to simulate spray gun physics (from: http://www.cd-adapco.com/products/star-ccm%C2%AE/lagrangiandem)	12
8	Power fit of cell base size vs. number of cells for mesh sensitivity test)	14
9	3 micrometer base size volume mesh (modified DiCarlo model design [15])	15
10	Isometric (left) and top (right) views of serpentine style microfluidic particle separators	17

11	Isometric (left) and top (right) views of second generation of devices .	18
12	Isometric (left) and top (right) view of third generation of device . . .	18
13	Isometric (left) and top (right) views of fourth generation of devices .	19
14	Isometric (left) and top (right) views of fifth generation of devices . .	20
15	Isometric (left) and top (right) views of fifth generation of devices . .	21
16	Problems with initial direct simulation of capture efficiency were due to fluid phase not reacting to the presence of a particle in the trapping passage. This caused particles to cluster around the trapping passage, which does not reflect what happens in experiments.	23
17	Volume fraction contour plot of DEM particles (top) compared to appearance of DEM particles in simulation (bottom). Notice the velocity contour of the fluid phase is not affected by a particle blocking the trapping passage. A more realistic simulation where the fluid is affected by the presence of a particle blocking the trapping passage is needed to directly simulate capture efficiency.)	24
18	PDMS poured over negative SU-8 mold on a 4-inch silicon wafer. . .	26
19	Successful particle capture in third generation device. While this device performed better than most in simulation, particle capture did not occur at some particle inlet positions.	27
20	Successful particle capture in fifth generation device. Again, while this device performed better than most in simulation, particle capture did not occur at some particle inlet positions.	28
21	Successful particle capture in fifth generation device. Particle capture occurred at all particle inlet positions in simulation for this particular design.	28
22	Top view of device that performed best in simulation	29
23	Fabricated device	30

LIST OF TABLES

1	Results of mesh sensitivity testing (percent difference is compared to 1 micrometer base size mesh)	14
---	--	----

ABSTRACT

OPTIMIZATION OF MICROFLUIDIC PARTICLE SEPARATOR GEOMETRY USING
COMPUTATIONAL FLUID DYNAMICS

JOSEPH PETERSEN

2018

Computational fluid dynamics software was used to simulate the motion of circulating tumor cells in a variety of microfluidic cell isolation devices. Design of several novel microfluidic cell isolation devices was aided by viewing streamlines of fluid in devices in simulation. Devices that performed best in simulation used 5-micrometer wide guiding channels to guide cells to the capture location in the device. While these devices performed better than other devices in simulation and captured all particles regardless of position along inlet, experimental results differ from simulation.

1 INTRODUCTION

1.1 DEFINITIONS

The following section contains a list definitions of abbreviations and nomenclature used in this thesis.

Computer Aided Design (CAD) - the use of computer systems and software to aid in design

Computational Fluid Dynamics (CFD) - uses numerical methods to solve fluid mechanics problems (usually involves the use if high powered computers)

Circulating Tumor Cell (CTC) - a cell that has broken off of a tumor and entered the vascular or lymphatic system.

Fill Factor - number of traps filled divided by the total number of traps in a cell trapping device

Microfluidics - involves the manipulation of fluid on a sub-millimeter scale

Polydimethylsiloxane (PDMS) - silicon elastomer used in the fabrication of many microfluidic devices. It is optically transparent and gas and vapor permeable.

Trapping Efficiency - number of trapped cells divided by minimum number of cells necessary to achieve a fill factor of 90 percent in a cell trapping device

1.2 OVERVIEW

Biological cells are the fundamental building blocks of all known living organisms. While much has been learned since the discovery of the cell in 1665, continuously developing better understanding of these basic units of life is an ongoing effort important to many scientific disciplines.

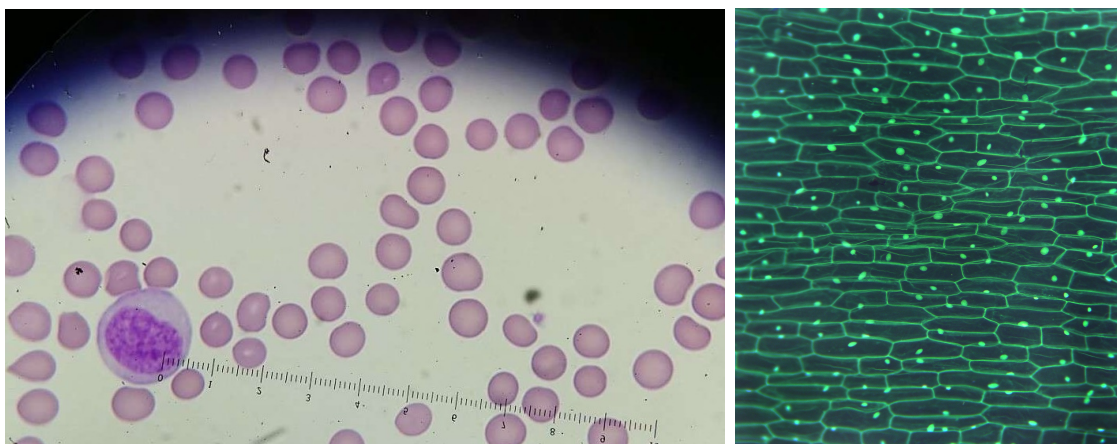


Figure 1: Cells perform a variety of functions for living organisms. For example, blood cells in the human circulatory system transport nutrients across the body (left), while plant cells (right) provide a rigid structure for the organism in addition to other critical functions.

For certain areas of research, it has become increasingly important to be able to observe individual cells that are isolated and separated from other cells. This is especially important for cancer research, where it is important to take the heterogeneity of cancer cell populations into account [1], [5], [7], [8], [10]–[12], [14]–[16]. Due to the small scale of cells, separating and isolating individual cells requires specialized equipment. Common accepted methods of cell isolation include flow cytometry and other similar methods that require significant monetary investment and a high level of training due to the complexity and cost of equipment [4], [5].

Many novel device designs have been proposed to remedy these issues. One promising type of device uses only hydrodynamic forces in micrometer scale channels to immobilize and isolate cells flowing through the device (Figure 2). These microfluidic devices offer significant advantages over the macro scale methods including low cost and simplicity of the devices, reduced consumption of reagents, and completely avoiding the use of relatively costly fluorescent antibodies [5]. However, these microfluidic devices have not yet been widely adopted in biological research or diagnostic studies due to their low capture efficiency, which limits their usefulness for isolating rare cells such as circulating tumor cells.

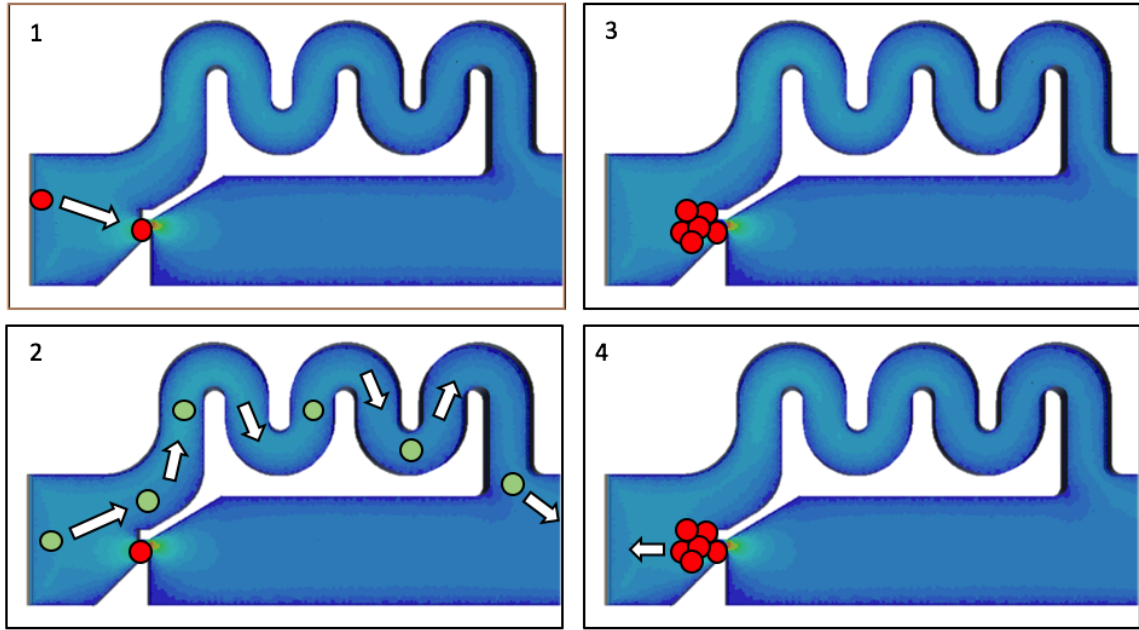


Figure 2: Cell is guided to trapping passage by hydrodynamic forces (1). Because the trapping passage is plugged, other cells are guided around the trapping passage thorough the longer serpentine passage to the next trap in the array (2). When trapping passages are full, cells are cultured (3). Cultured cells are then removed from device for study (4).

1.3 THESIS CONTRIBUTIONS

The goal of the proposed design process is to create a microfluidic device with improved capture efficiency that uses only hydrodynamic forces in microchannels to isolate cells.

This novel device should be of value to researches by providing a low cost and effective method of capturing rare cells. Improved capture efficiency compared to other microfluidic devices could drastically improve the usefulness of this technology.

Numerical simulation tools, particularly computational fluid dynamics (CFD) software, were used to guide the design process and allowed for rapid prototyping of device designs.

The principal contributions of this thesis are the development of computational fluid dynamics simulations using commercially available software involving the use of discrete element method particles to model the motion of micro-scale particles in a hydrodynamic cell isolation device, and the development of several novel hydrodynamic

cell isolation devices.

1.4 CELL SEPARATION AND ISOLATION

Most plant and animal cells range in size from 1 to 100 micrometers and are only visible under a microscope. Due to their small scale, it is a technical challenge to physically sort and isolate individual cells according to their properties. Most cell separation methods sort cells based on physical or chemical differences between cells. For example, cells can be sorted based on properties such as size, dielectric potential, or buoyancy [5].

1.4.1 RARE CELL CAPTURE AND ISOLATION

Pratt et al. provide an in depth look into various methods of rare cell capture in microfluidic devices. [7] Many microfluidic devices have been proposed to be used for the capture and isolation of rare cells. Overall there are two main types of designs that have been proposed. Serpentine traps take advantage of different flow resistances of varying microchannel lengths to capture and isolate cells flowing through the device. [15] Dicarolo traps use an array of cup shaped traps to more gently capture cells. [15]

1.4.2 CIRCULATING TUMOR CELLS

Circulating tumor cells are found in the blood vessels and lymphatic system of patients with epithelial tumors. These cells shed off of tumors and enter into the circulatory system where they act as seeds for new tumors. This is one way that cancer can spread through a patient. Disease progression and treatment effectiveness in a patient can be monitored by enumerating CTCs from a blood sample. A blood test is much less invasive than other ways of monitoring metastatic disease progression such as tissue biopsy. CTCs are relatively rare (1 -10 CTCs in a mL of blood in patients with epithelial tumors)[6] compared to other cells found in blood even in patients with advanced metastatic disease. This rarity contributes to the technical challenge of cell separation and isolation [2].

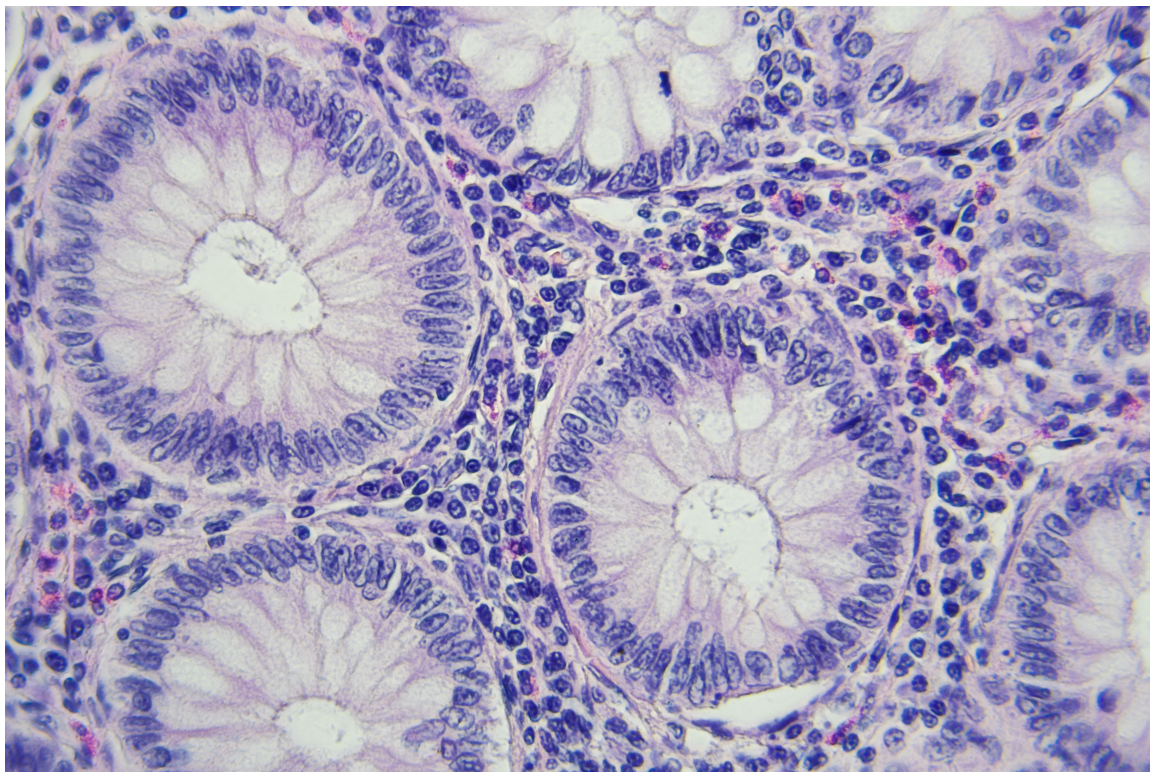


Figure 3: Cells in a tumor of human colon tissue at 400X magnification. Tumors of epithelial tissue have the potential to shed into the circulatory system and become CTCs.

1.4.3 CELLSEARCH® CTC TEST SYSTEM

CELLSEARCH® is a system for the detection, isolation, and enumeration of CTCs from a blood test. It uses immunomagnetic technology and fluorescence imaging to detect CTCs. It is currently the only FDA approved system of its kind. The test requires a 7.5 ml blood sample. [9]

1.4.4 MICROFLUIDIC PLATFORMS FOR CTC ISOLATION

1.5 MICROFLUIDICS

Many of the cell separation methods based on both physical and chemical properties can be scaled down to sub-millimeter scale. In addition to reducing the amount of sample and reagent required, micro-scale platforms for CTC isolation also have the advantage of array



Figure 4: The CELLSEARCH® System for identification, isolation, and enumeration of circulating tumor cells from a simple blood test.

format.

Sackmann et al. provide a general overview of early microfluidic technology and its impact in biology and medical research [10]. They conclude that over the past decade the number of articles about microfluidic technology has steadily increased, most articles are still published in engineering journals versus biology or multidisciplinary journals. They bring up the importance of making emerging technology easily used by the end user (in this case biology and medical researchers) for it to be widely adopted. They also explain that early microfluidic devices were fabricated out of silicon and glass due to the accessibility of these materials in clean rooms. However, most prototype microfluidic devices are now made of PDMS. There are some problems with PDMS, including barriers to using it as a material in large scale manufacturing. PDMS has also been shown to absorb some small molecules, which could lead to problems with some cell signaling experiments.

Volpatti et al. also provide an interesting perspective of the general microfluidics

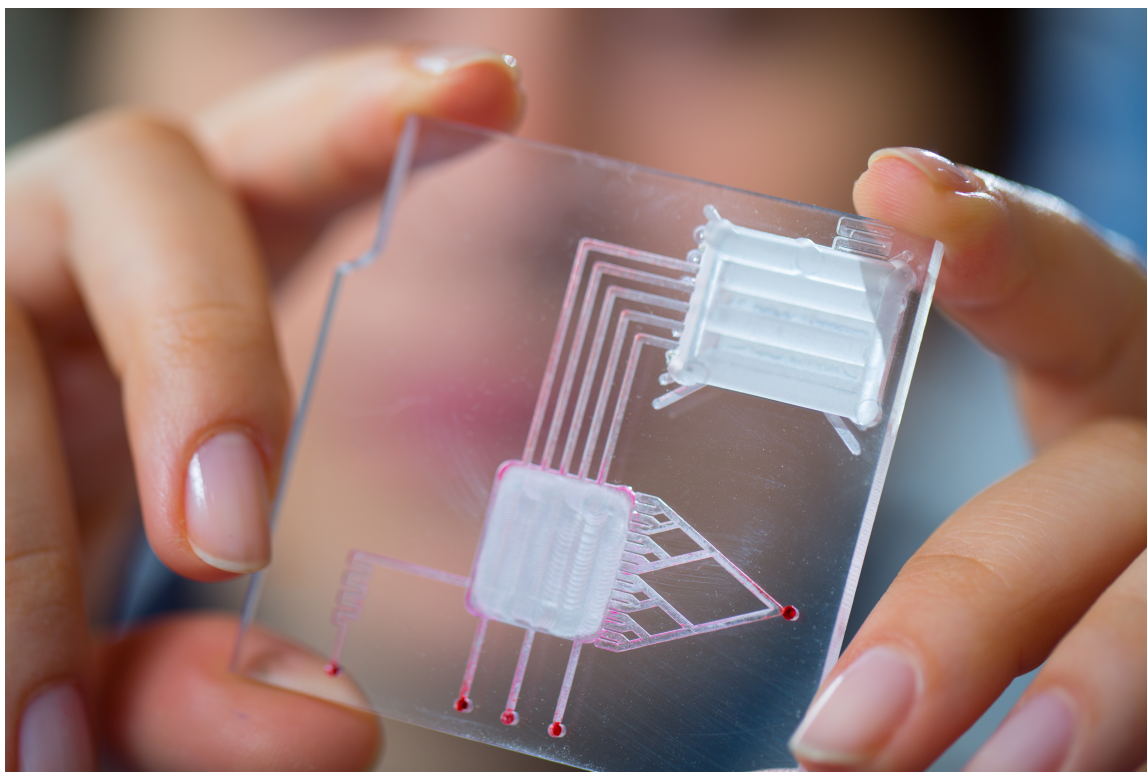


Figure 5: Microfluidic devices scale down the processes of laboratory equipment to sub millimeter scale.

market [13]. The microfluidics market is growing at a rate of 18-29% annually, and was valued at \$1.6 billion in 2013, however there are many challenges in bringing this new technology from an academic research setting to commercialization. One challenge that was mentioned is standardization. While PDMS is a common choice of material for prototyping microfluidic devices in an academic setting, using other materials such as poly methyl methacrylate (PMMA) and polycarbonate is recommended, as these materials are easier to manufacture in scale. Another challenge that was mentioned was that of integration. A given example of an integration problem is that many microfluidic platforms require the use of external pumping equipment and other hardware and software that is not user friendly.

Halldorsson et al. go into detail of the challenges and advantages of using PDMS in microfluidic devices and many other related topics.[3] There are many advantages to using a microfluidic platform for cell culture versus traditional methods. One of the main

problems that arises from using macroscopic methods for cell culture is that measurement are an average of the whole cell population being measured, as macroscopic cell cultures usually contain more than 1000 cells. The ability to isolate individual cells would enable researchers to study many things that are dependent on the heterogeneity of the individual cells. Also mentioned is the goal of creating an array of microfluidic devices that mimic the function of entire organs. While this is a far off goal, creating a platform like this would be revolutionary for many applications such as drug testing. Efforts to combine microfluidic platforms to create this synthetic "organ-on-a-chip" are already under way. Although there are many advantages to culturing cells in a microfluidic chip, the micro-scale environment presents a few challenges when compared to traditional culture methods. One challenge is that of different materials used in the fabrication of micro-scale devices. As mentioned in the previous section, PDMS is commonly used because it is easily molded using soft lithography. While medical grade PDMS is generally considered to be biocompatible and not cytotoxic, not all types of cells will grow on PDMS the same way that they do on macroscopic culture plastics. Some of these problems could be avoided by treating the surface of PDMS with a serum or a concentrated protein solution. Another problem that could possibly arise from the use of PDMS in cell culture devices is that if the curing process is not completed correctly, uncrosslinked polymers may be left within the material. These uncrosslinked polymers may leach out of the material and into culture cell membranes. Another potential problem of using PDMS in a cell culture device is that PDMS is hydrophobic. While traditional plastics used in macroscopic culture can be surface treated with oxygen plasma or UV treatments to decrease hydrophobicity, PDMS will revert back to a hydrophobic state over time. This can also be remedied by using a surface treatment of charged molecules or extracellular matrix proteins such as fibronectin, collagen or laminin. Another problem of using PDMS arises from its porous nature. Small molecules may leach into the PDMS which can affect the results of many types of experiments. Again, using a surface treatment can help with this issue in some

cases. PDMS is also permeable to gases, which means that water is able to evaporate through it. Cell culture medium osmolarity could be affected by this evaporation, so it should be kept to a minimum. Using covers on the device may be necessary if evaporation causes issues with cell culture. The transition to micro-scale wells from macroscopic culture may create some problems with nutrient consumption and culture medium turnover. Generally, cells cultured in a microfluidic platform will require more nutrients and a higher rate of medium turnover than those cultured using macroscopic methods.

1.6 COMPUTATIONAL FLUID DYNAMICS

Computational fluid dynamics (CFD) involves the use of numerical methods to solve the navier-stokes equations for the visualization of fluid flow problems. The Navier-Stokes equations can be used to describe how the velocity, pressure, temperature, and density of a fluid are related.

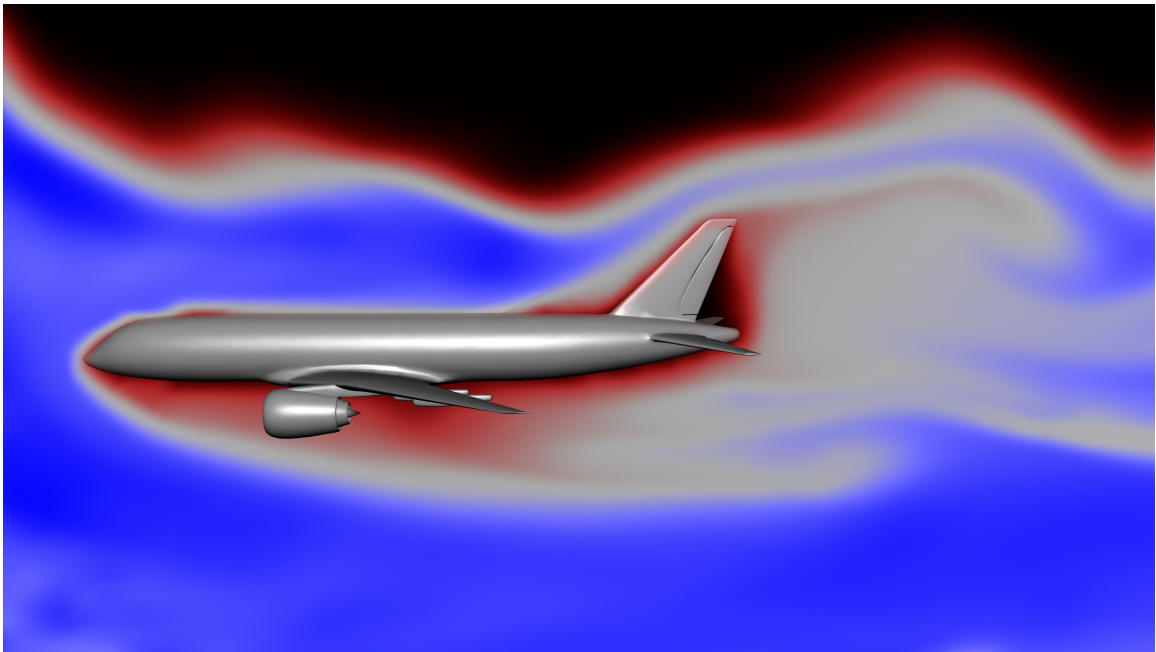


Figure 6: Computational fluid dynamics is used simulate and visualize the flow of fluid around objects, and in some cases can substitute for costly experimental tests.

1.6.1 THE NAVIER-STOKES EQUATIONS

Equations 1 and 2 are the continuity and conservation of momentum equations used in computational fluid dynamics. The Navier-Stokes equations can be used to describe fluid properties in three spatial dimensions, and are shown here using compact Einstein notation.

The continuity equation ensures that mass is conserved for a fluid flow. The incompressible continuity equation is shown in Equation 1.

$$\frac{\partial u_i}{\partial x_i} = 0 \quad (1)$$

Momentum must also be conserved for a given fluid flow. The incompressible momentum equation that governs this is shown in Equation 2.

$$\frac{\partial(u_i)}{\partial t} + \frac{\partial(u_i u_j)}{\partial x_j} = \left(-\frac{\partial P}{\partial x_i} + \frac{\partial \tau_{ij}}{\partial x_j} \right) \rho \quad (2)$$

The following is a list of variables used to describe fluid properties in Equations 1 and 2:

x = position

u = velocity

t = time

P = pressure

τ = shear stress

1.6.2 DISCRETE ELEMENT METHOD

The discrete element method (DEM) uses numerical methods to simulate solid particle dynamics. It is very similar to molecular dynamics but includes rotational degrees of freedom and stateful contact. It is possible to simulate particles of complex shape using

polyhedral geometry. Discrete element particle modeling has a variety of applications, including modeling solutions in a liquid, flow of granular materials such as sand, flow and sedimentation of bulk materials in storage containers, and mechanics of fine powders. It is widely used to simulate rock and powder flows.

Equation 3 describes how momentum is conserved for particles in a DEM simulation.

$$m_p \frac{\partial u_p}{\partial t} = F_s + F_b \quad (3)$$

Where:

m_p = particle mass

u_p = particle velocity

t = time

F_s = sum of surface forces acting on the particle

F_b = sum of body forces acting on the particle

Angular momentum must also be conserved for a DEM simulation. Equations 4 and 5 describe how angular momentum is conserved for DEM particles.

$$\frac{d}{dt}(I_p \omega_p) = \sum_{Particles} L + \sum_{Boundaries} L \quad (4)$$

$$L = r(F_c + c_r n_c \frac{\omega_p}{|\omega_p|}) \quad (5)$$

Where:

I_p = particle moment of inertia

ω_p = particle angular velocity

t = time

L = angular momentum

r = particle radius

F_c = contact force

c_r = coefficient of rolling friction

n_c = number of contacts

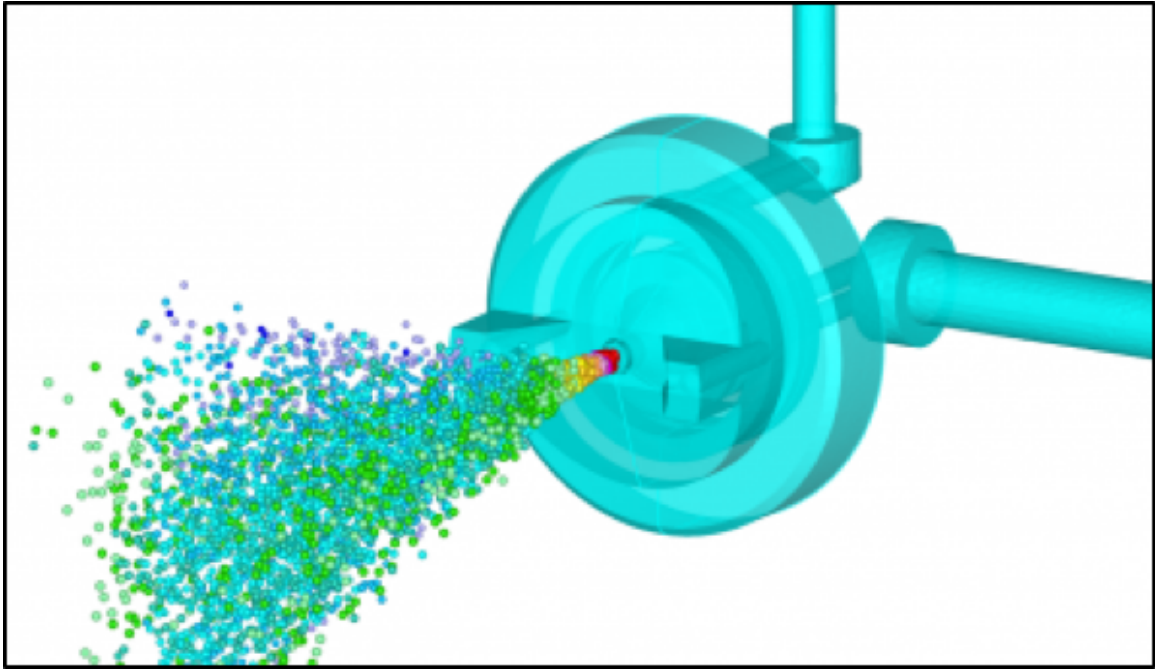


Figure 7: DEM objects used to simulate spray gun physics (from: <http://www.cd-adapco.com/products/star-ccm%C2%AE/lagrangian-dem>)

The DEM method has been expanded into the extended discrete element method which allows DEM to be coupled to CFD continuum. The ability to couple DEM to CFD allows many interesting engineering problems to be simulated. One of these problems is simulating the path of biological cells (as DEM particles) in fluid flowing through a microfluidic cell trapping device (as CFD continuum). To successfully simulate this, the DEM particles must be affected by the flow of the fluid flowing in the device, and the fluid flowing in the device must be affected by the DEM particles. This two way coupling is much more computationally expensive than one way coupling, but since the number of particles is minimal for this type of simulation (generally fewer than 100 particles in the device at any time step), the use of high power computers is not required for this specific

case.

1.6.3 STAR-CCM+

Star-CCM+ is a CFD software developed by CD-Adaptco. CD-Adaptco was acquired by Siemens in April 2016 for 970 million usd. CCM stands for "computational continuum mechanics". The software was developed from the start to be able to simultaneously solve fluid flow and heat transfer problems, in addition to the ability to perform a variety of multiphase simulations.

2 METHOD

2.1 MESH

Because this project involved repeating similar simulations, it was worthwhile to investigate the optimal mesh base size. While many simulations become more accurate as mesh base size decreases, the addition of DEM particles in the simulation complicates matters. In a simulation that includes DEM particles, a mesh base size that is smaller than the diameter of the particles can lead to some non physical results.

The surface mesher, polyhedral mesher, and extruder meshing tools were used in Star-CCM+ to generate surface and volume meshes for this project. 6 simulations were performed to test the effect of mesh base size on a steady state simulation without particles. This was done to minimize computation time while maintaining appropriate accuracy for future simulations. Results indicated that a simulation with a mesh base size of 3 micrometer and 98,037 cells yields only a 2.80% difference in the maximum velocity of a simulation with a base size of 1 micrometer and 2,208,096 cells. Further results of mesh sensitivity testing are shown in Table 1 and Figure 8. Views of a 3 micrometer base size mesh are found in Figure 9.

Mesh Base Size (m)	Number of Cells	Maximum Velocity (m/s)	Difference
5.00E-06	29486	0.043820	4.50%
3.00E-06	98037	0.044572	2.80%
2.00E-06	312353	0.044373	3.25%
1.75E-06	427443	0.043975	4.15%
1.25E-06	1102561	0.045277	1.23%
1.00E-06	2208096	0.045837	0.00%

Table 1: Results of mesh sensitivity testing (percent difference is compared to 1 micrometer base size mesh)

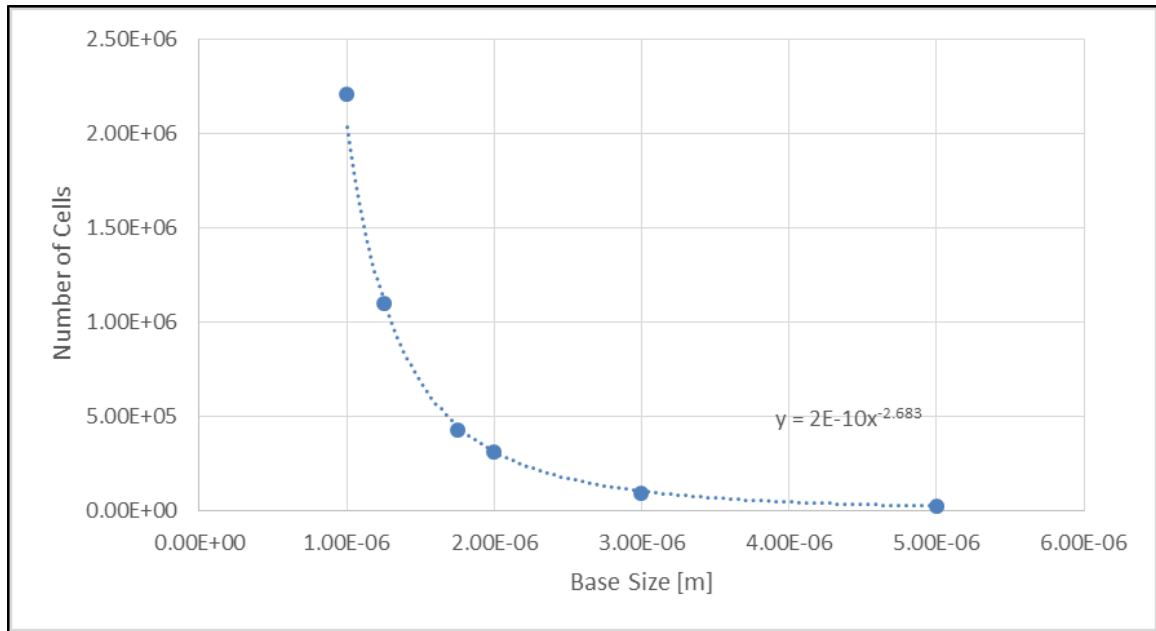


Figure 8: Power fit of cell base size vs. number of cells for mesh sensitivity test)

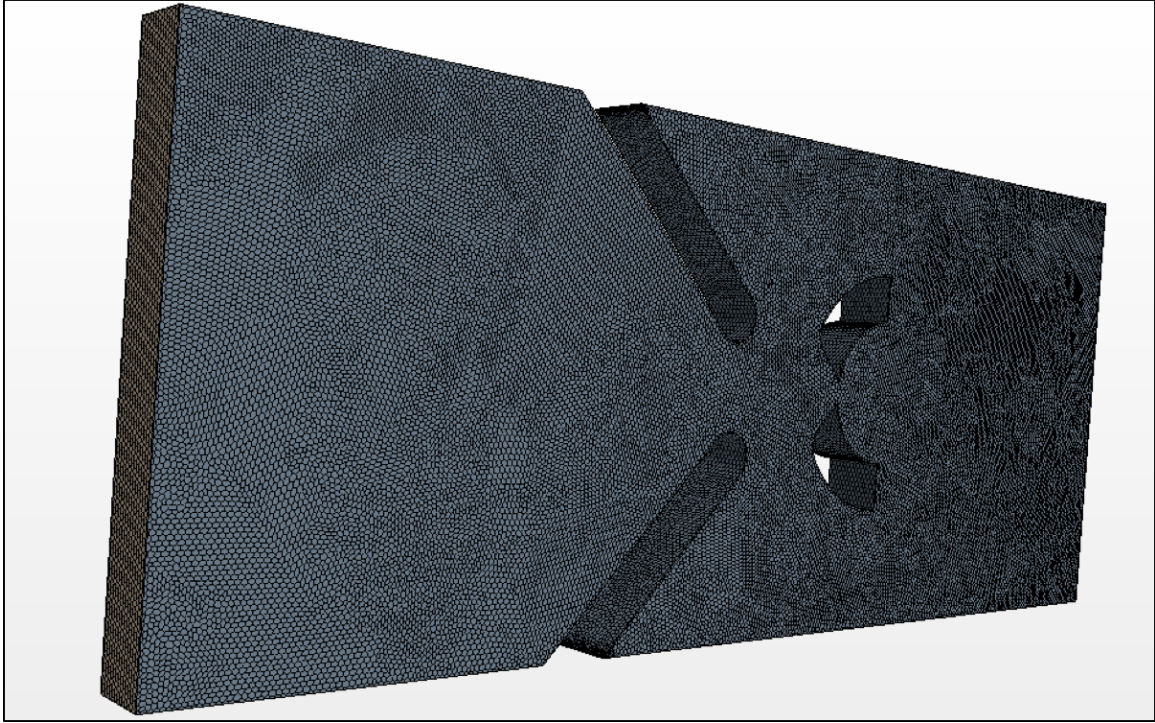


Figure 9: 3 micrometer base size volume mesh (modified DiCarlo model design [15])

2.2 PHYSICS MODELS

Maximum Reynolds number for highest velocity and maximum hydraulic diameter found in a device was calculated to determine whether turbulence modeling was required for the fluid phase in simulation using Equations 6 and 7:

$$D_h = \frac{2ab}{a + b} \quad (6)$$

Where:

D_h = hydraulic diameter

a = rectangular duct width

b = rectangular duct height

$$Re_{max} = \frac{v_{max} D_h}{\nu} \quad (7)$$

Where:

Re_{max} = maximum Reynolds number

v_{max} = maximum fluid velocity

ν = fluid kinematic viscosity

Maximum design parameters were input into Equations 6 and 7 to determine whether flow is laminar or turbulent in the devices, as shown in Equations 8 and 9:

$$D_h = \frac{2(2.5 \times 10^{-5} m)(4.0 \times 10^{-5} m)}{2.5 \times 10^{-5} m + 4.0 \times 10^{-5} m} = 3.08 \times 10^{-5} m \quad (8)$$

$$Re_{max} = \frac{(0.005 m/s)(3.08 \times 10^{-5} m)}{1.12 \times 10^{-6} m^2/s} = 0.137 \quad (9)$$

The Reynolds number will vary between different designs due to different geometries and flow rates, but this calculation confirms laminar flow due to Reynolds number being many orders of magnitude lower than the Reynolds number of turbulent flows. Thus, no turbulence modeling was used in the fluid phase of simulations.

15-micrometer diameter spherical DEM particles were used to model CTCs in simulations. Interaction between the walls of the device and DEM particles was modeled using particle-wall interaction. The drag force that the fluid phase exerts on the DEM particles was also modeled.

2.3 MODEL DEVELOPMENT

Several novel microfluidic particle separator designs were developed to be tested in simulation. Figure 10 shows the first generation of novel designs that are based on existing serpentine stye traps. Positive CAD model geometry is where fluid phase flows through the devices in the following figures.

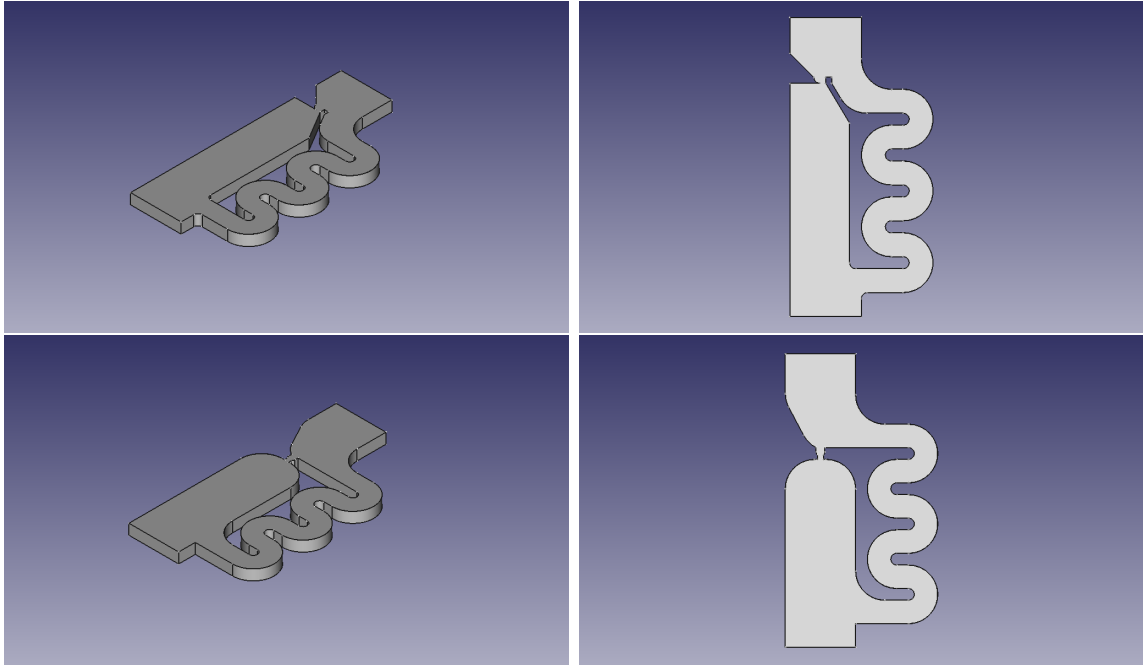


Figure 10: Isometric (left) and top (right) views of serpentine style microfluidic particle separators

The second generation of device designs aimed to improve capture efficiency compared to the first generation serpentine style designs. The fluid streamlines in simulation were viewed and geometry was modified near the trapping portion of the device so particles are forced closer to traps (Figure 11).

Another attempt was made to optimize capture efficiency after looking at the streamlines of the second generation of devices. The resulting device geometry is shown in Figure 12.

The fourth generation of devices used multiple fluid inlets to guide particles to the trapping portion of the device. These designs are shown in Figure 13.

Lastly, the fifth generation of devices used an single fluid inlet with guiding channels between two channels to guide particles to the trapping portion of the the device. Another advantage of having these guiding channels is that they reduce pressure exerted on trapped particles due to fluid flow through the device. These designs are shown in Figures 14 and 15.

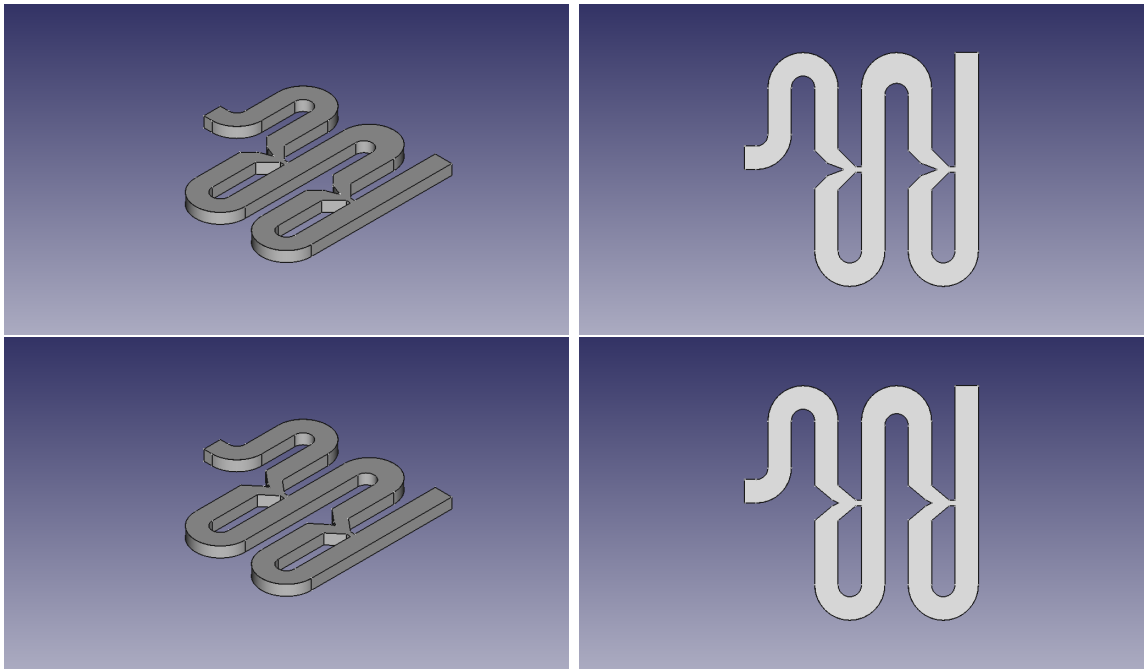


Figure 11: Isometric (left) and top (right) views of second generation of devices

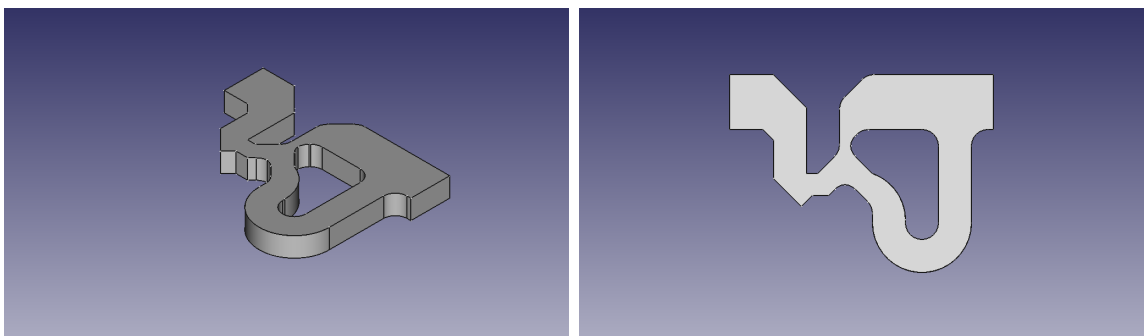


Figure 12: Isometric (left) and top (right) view of third generation of device

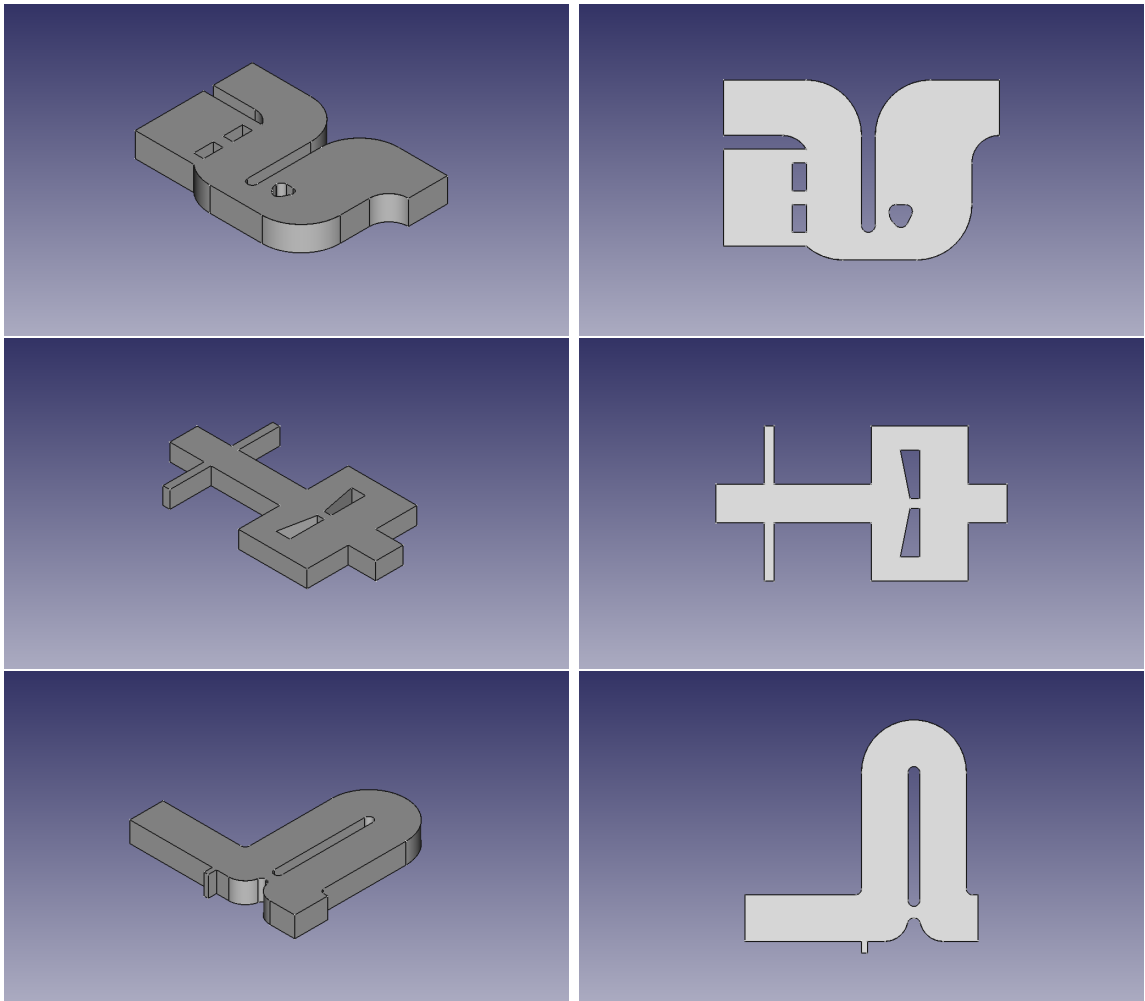


Figure 13: Isometric (left) and top (right) views of fourth generation of devices

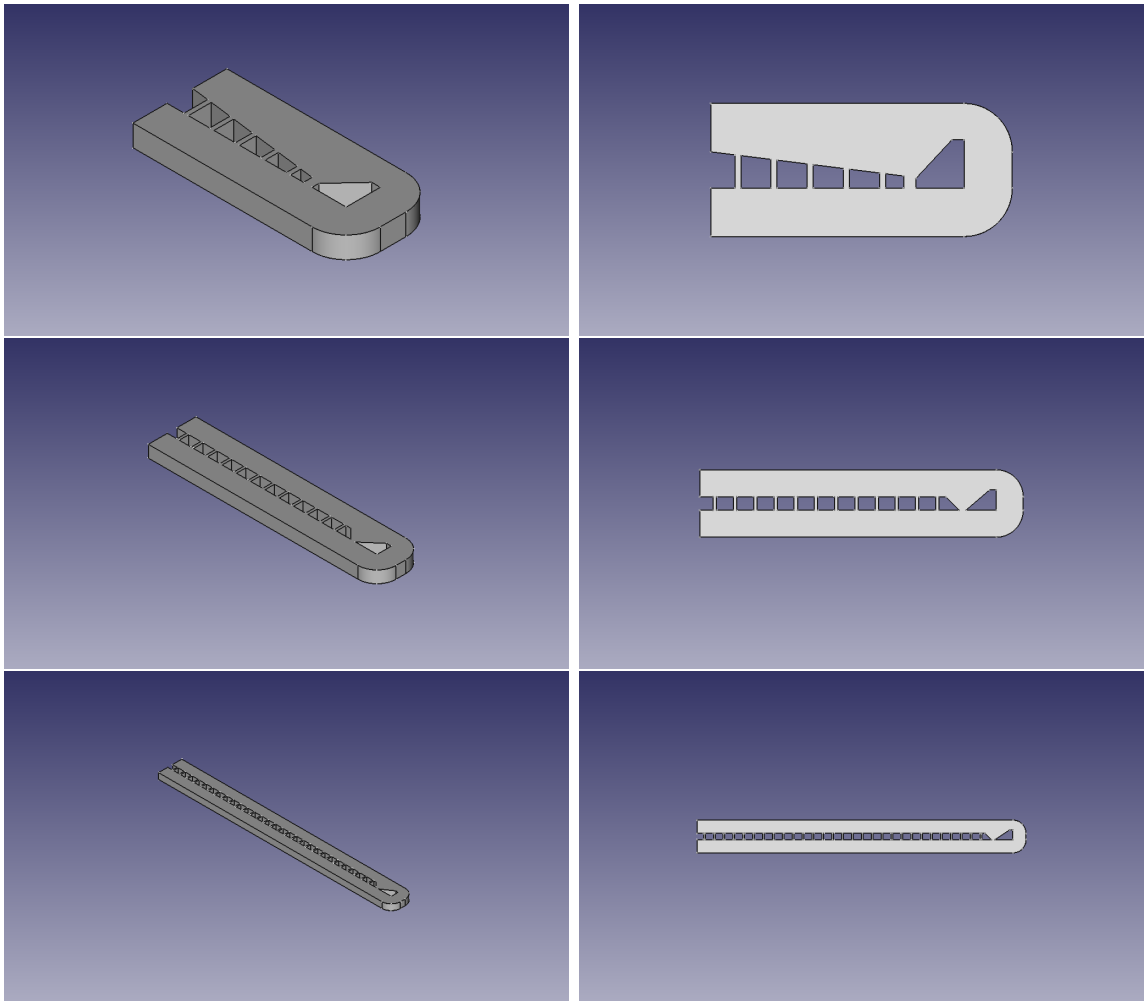


Figure 14: Isometric (left) and top (right) views of fifth generation of devices

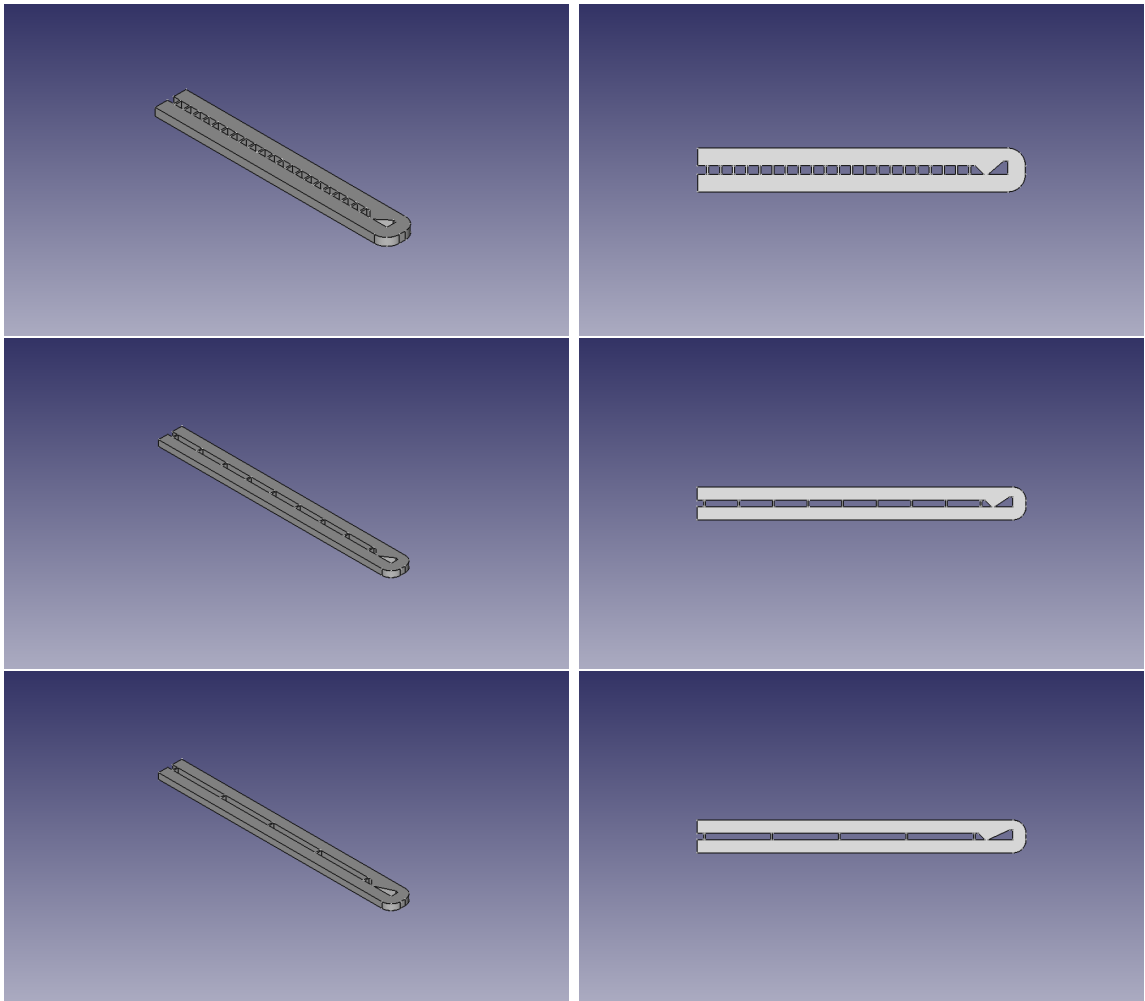


Figure 15: Isometric (left) and top (right) views of fifth generation of devices

2.4 PROOF OF CONCEPT MODEL

Initially, a few proof of concept simulations using rough device geometry were performed to determine whether DEM particles coupled with CFD would be suitable to determine capture efficiency in microfluidic particle separators. Existing device geometry with published results were modeled using CAD software, and simulation results were compared to published results.

While the proof of concept simulations appear to provide an accurate representation of fluid and particle dynamics in a microfluidic particle separator, there are a few problems with the models that reduce their usefulness. One example is that the DEM particles do not plug the trapping portion of the device and stop fluid from flowing. These non physical results make determining the capture and trapping efficiency of devices impossible in this particular type of simulation. Also, this makes simulation of a full array of traps impossible until the dynamics of particles in the trap can be effectively modeled.

Figures 16 and 17 contains a detailed explanation of what is happening to cause the aforementioned issues with the proof of concept model.

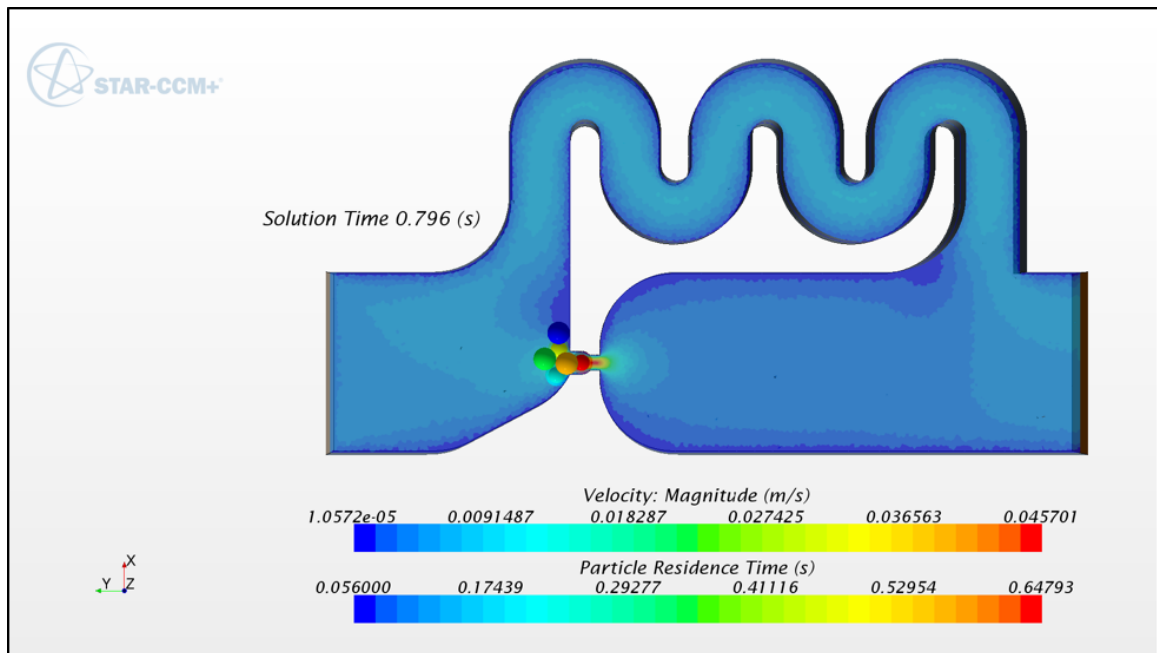


Figure 16: Problems with initial direct simulation of capture efficiency were due to fluid phase not reacting to the presence of a particle in the trapping passage. This caused particles to cluster around the trapping passage, which does not reflect what happens in experiments.

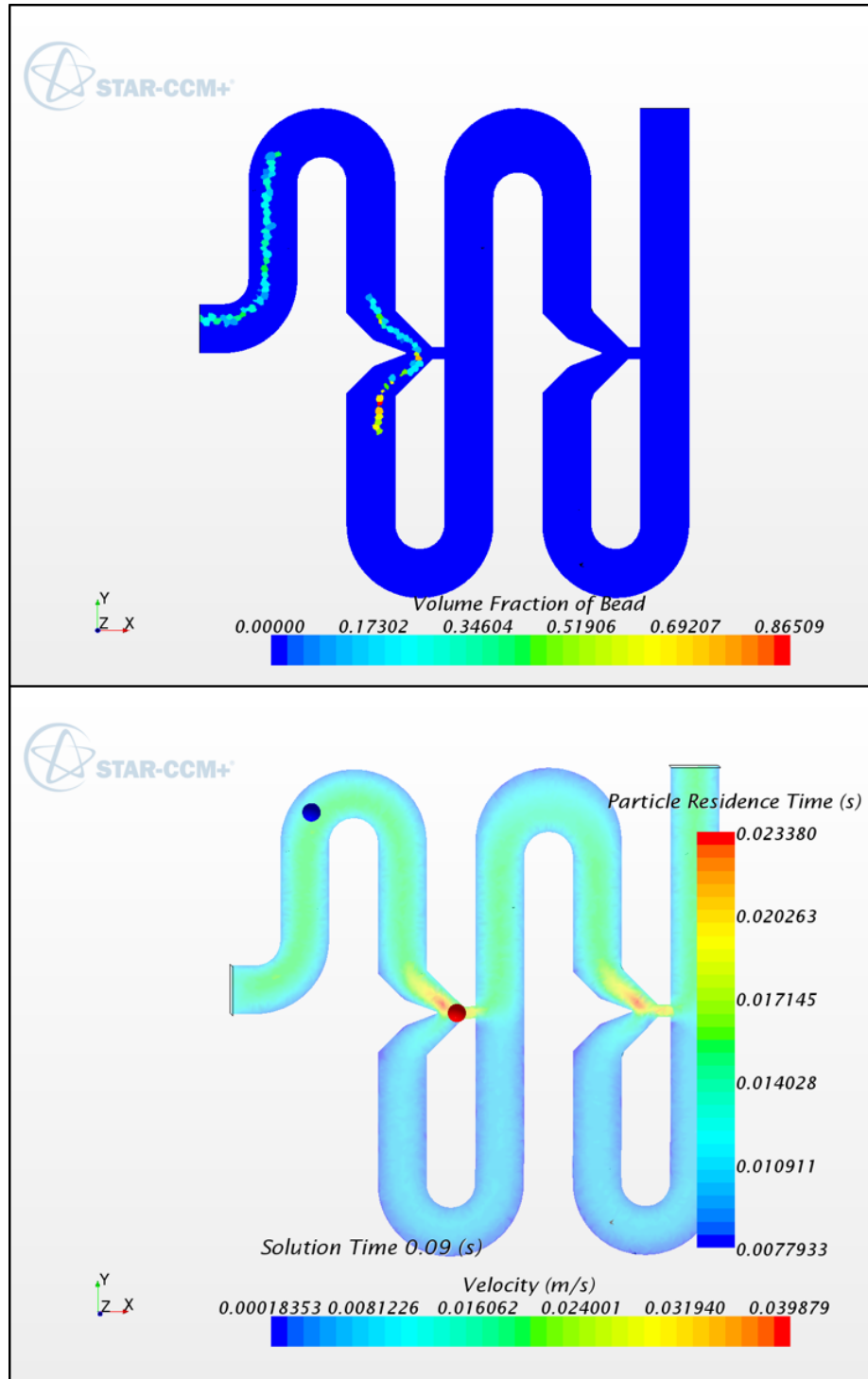


Figure 17: Volume fraction contour plot of DEM particles (top) compared to appearance of DEM particles in simulation (bottom). Notice the velocity contour of the fluid phase is not affected by a particle blocking the trapping passage. A more realistic simulation where the fluid is affected by the presence of a particle blocking the trapping passage is needed to directly simulate capture efficiency.)

2.5 SINGLE DEM PARTICLE SIMULATION

To work around the limitations discussed in the previous section, a single particle simulation approach was developed. In this approach, the path of a single DEM particle is observed in a single hydrodynamic cell trap well. The simulation is run multiple times, each time moving the initial position of the particle along the inlet so that a full range of possible inlet positions is simulated.

This approach has several advantages over the more direct approach of simulating an entire array of particle traps with multiple DEM particles. First, the computational cost of the single particle simulation is much lower than the direct simulation. This is due to only having to simulate a single particle versus multiple particles, and a single trap versus an entire array. Simulating a large number of DEM particles is computationally expensive. Also, two-way coupling is not needed for this type of simulation.

2.6 DEVICE FABRICATION

A negative photoresist SU-8 mold of the device geometry was fabricated using soft photolithography. The SU-8 photoresist was spun on a 4-inch silicon wafer. The wafer was placed on a hotplate set at 65°C for 3 minutes and then placed on a hotplate set at 95°C for 8 minutes. Then, the wafer was exposed to UV light using a mask aligner. After exposure the wafer was placed on the hotplate set at 65°C for 1 minute, then on the hotplate set at 95°C for 6 minutes. The uncrosslinked SU-8 was then removed from the mold by washing with SU-8 developer for 5 minutes. The thickness of the SU-8 mold was 30 micrometer.

Polydimethylsiloxane (PDMS) was then poured over the mold and allowed to set overnight (Figure 18). The PDMS device was peeled off from the mold and 1 mm holes for the inlet and outlet tubes were punched through the PDMS. Finally, the PDMS was bonded to a glass slide using corona discharge (25 seconds for both the glass and PDMS surface), and 1 mm inlet and outlet tubes were fit into the punched inlet and outlet holes.

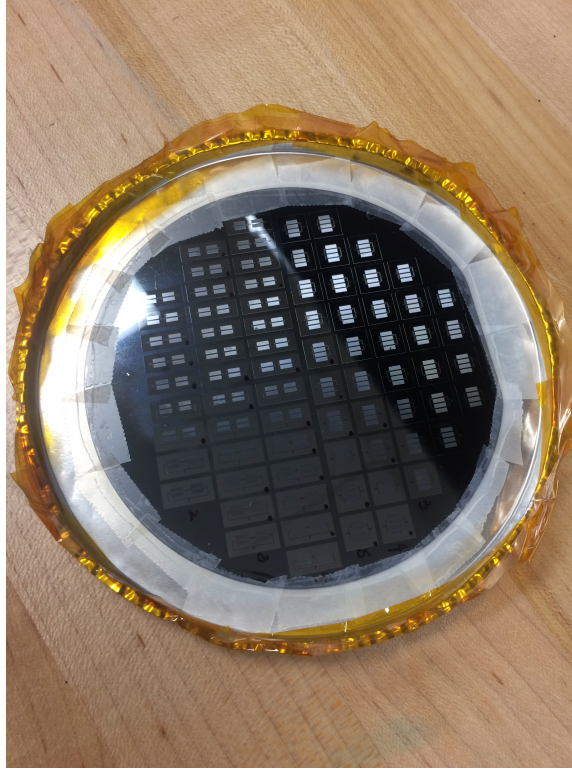


Figure 18: PDMS poured over negative SU-8 mold on a 4-inch silicon wafer.

3 RESULTS

3.1 SIMULATION RESULTS

All device designs mentioned in the Model Development section were tested in simulation as described in the Single Particle Simulation section. Figures 19 - 21 show notable simulation results. The position of the particles in these figures represents the steady state position of the particle for the selected simulation. Also note that color intensity represents fluid velocity of the middle cross section of the device.

The microchannel geometry that produced the most consistent DEM particle capture in simulation utilized small guiding channels between microchannel rows to guide particles to capture location. The microchannel geometry is shown in Figure 21. This optimized microchannel geometry in simulation was able to isolate and immobilize particles for all channel inlet positions for the specified flow rate of fluid through the

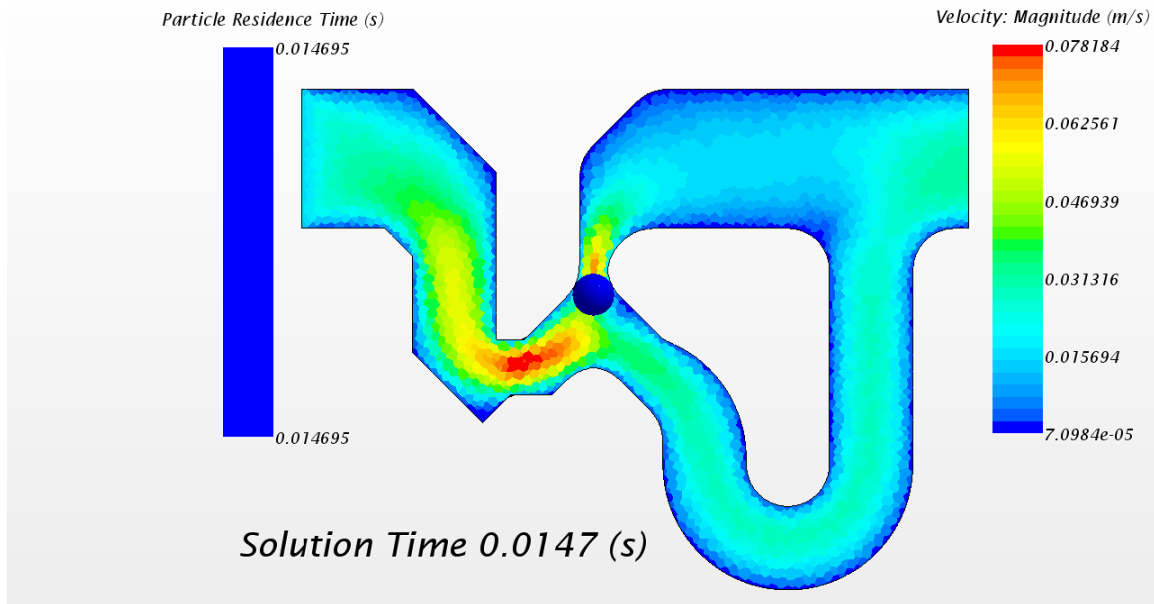


Figure 19: Successful particle capture in third generation device. While this device performed better than most in simulation, particle capture did not occur at some particle inlet positions.

device. This proposed device performs much better than other devices when using the simulation results to compare capture efficiency rates.

To verify the results of the simulation, an experiment using the proposed device was performed as described in the Experimental Results section. The experimental data was compared to the data from the simulation and used to further adjust and optimize simulation parameters.

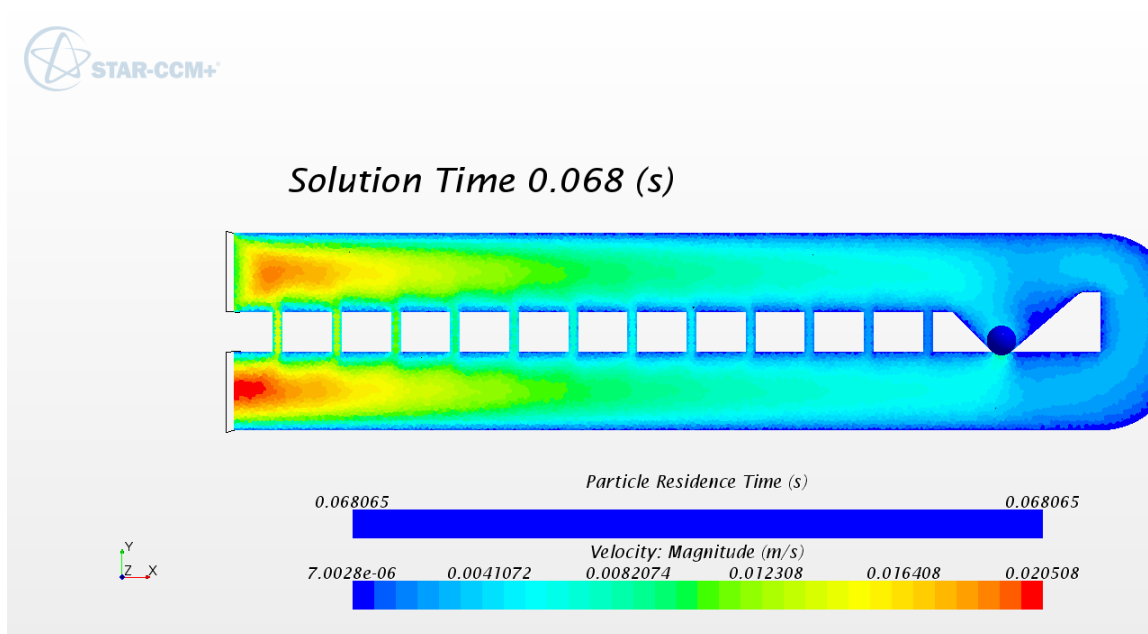


Figure 20: Successful particle capture in fifth generation device. Again, while this device performed better than most in simulation, particle capture did not occur at some particle inlet positions.

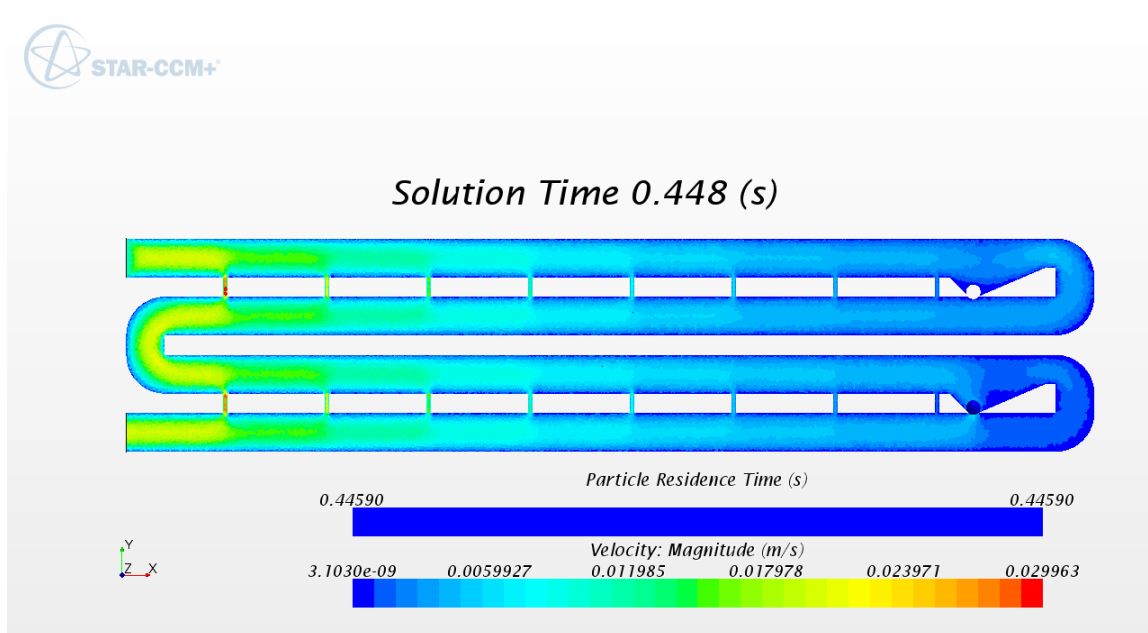


Figure 21: Successful particle capture in fifth generation device. Particle capture occurred at all particle inlet positions in simulation for this particular design.

3.2 EXPERIMENTAL RESULTS

Arrays of the device design that performed the best in simulation (Figure 22) was fabricated as described in the Device Fabrication section.

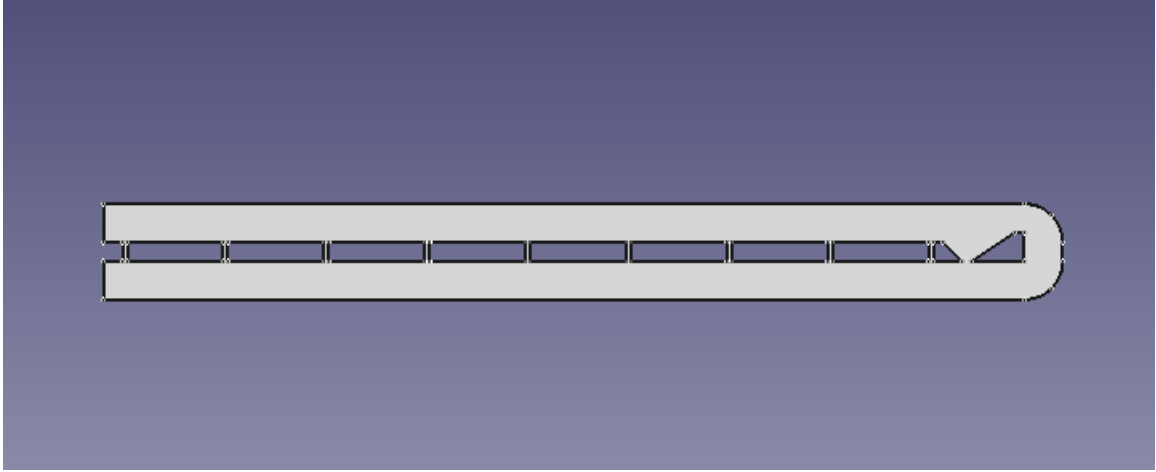


Figure 22: Top view of device that performed best in simulation

While the device array did successfully capture and isolate many 15-micrometer diameter microbeads, there were notable differences between simulation. In simulation, the device captured particles at all inlet positions. In experiment, some devices in the array successfully captured particles, while others did not. Another difference between simulation and experiment was that in experiment, particles had a tendency to get trapped in the guiding channels between the main channels of the device; this did not ever occur in simulation.

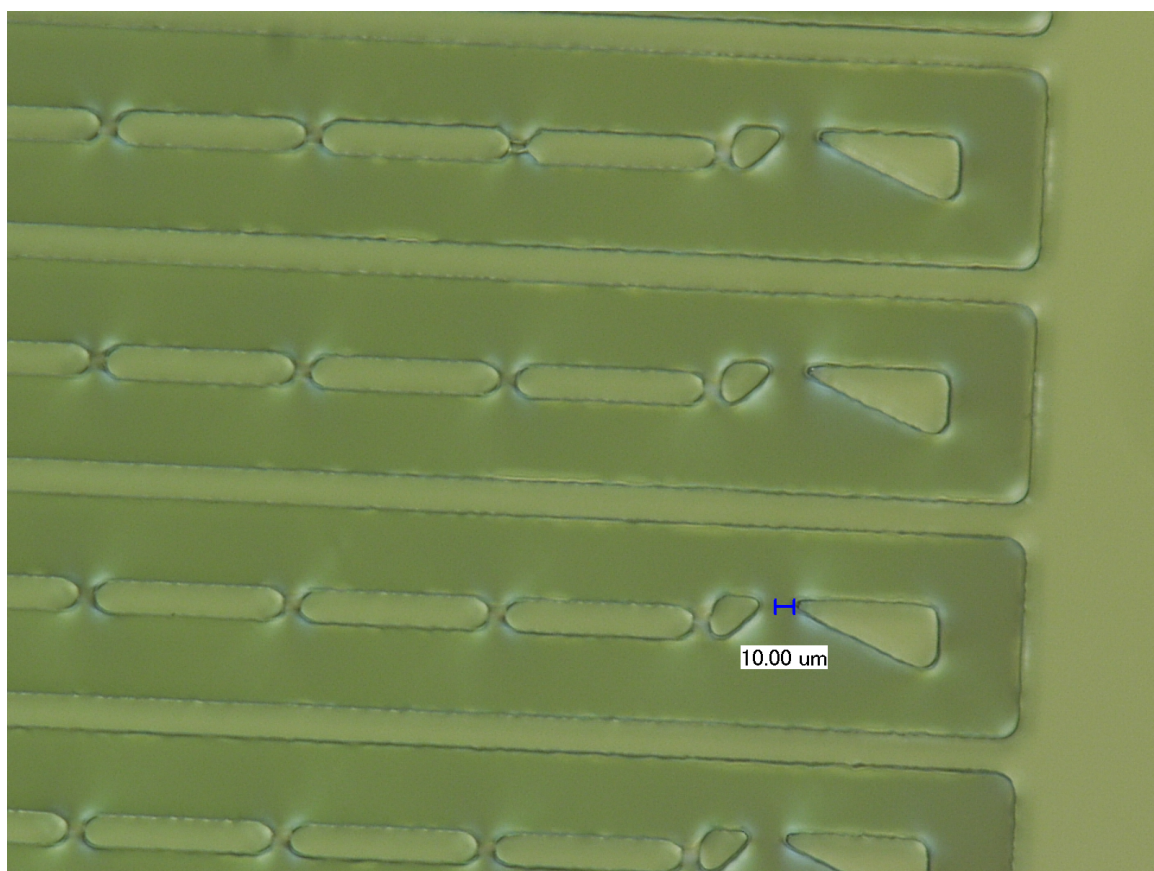


Figure 23: Fabricated device

4 INTERPRETATION

There are a few limitations of the simulation used in the described design process. For example, only a single spherical DEM particle is modeled in each simulation, where in reality many particles of varying size and shape will be present in the microchannel at any given time. Also worth noting is that the device will consist of an array of the proposed microchannels. The amount of time a specified volume of liquid will take to flow through this array of microchannels at a specific fluid flow rate is difficult to determine from simulation because only a single microchannel is simulated.

As described in the previous section, there were many differences between simulation and experimental results. Some of these differences are minor and do not detract from the usefulness of the simulation, however some drastically reduce the usefulness of the simulation. Experimental validation of numerical simulation is essential to prove the validity and usefulness of the simulation.

Even with these limitations, the simulation can be useful to determine pressure drop across a single microchannel and extrapolate this data to determine the pressure drop across an array of devices. If pressure drop across the array of microchannels exceeds the strength of the bond between the PDMS and glass, the device will burst when fluid is pumped through. The pressure exerted on a trapped particle in the device must also be considered, as cells can be damaged if they are exposed to high pressure gradients.

The simulation failed to effectively determine capture efficiency of a novel microfluidic particle trapping device. The following section discusses causes of differences in results of simulation versus experiment.

4.0.1 CAUSES OF DIFFERENCE BETWEEN SIMULATION AND EXPERIMENT

As discussed in the Proof of Concept section, the position of DEM particles is calculated by calculating a volume fraction of solid phase in the meshed cells of the fluid phase. This

is suitable for simulations where the size of the particles is much smaller than the fluid cell base size, but nonphysical results occur when the size of the particles is close to the fluid cell base size.

Another source of error could be the resolution of the equipment used to fabricate the physical device. As with any fabrication process the sharpness of corners and edges will depend on the resolution of the equipment used. Its possible that a device fabricated using higher resolution equipment would affect the flow of fluid differently than the device used in experiment.

5 CONCLUSION

To conclude, CFD simulations were used to simulate cell capture in hydrodynamic cell isolation device microchannels. The simulation aided in the design of a novel microfluidic cell isolation device that uses small guiding microchannels to guide cells to the capture location in the device. While this device performs better than other devices in simulation, experimental validation is required before more conclusions are drawn. Future work will include this experimental validation and further optimization of the simulation parameters and device geometry.

REFERENCES

- [1] D. Di Carlo, N. Aghdam, and L. P. Lee, "Single-cell enzyme concentrations, kinetics, and inhibition analysis using high-density hydrodynamic cell isolation arrays," *Analytical chemistry*, vol. 78, no. 14, pp. 4925–4930, 2006.
- [2] I. J. Fidler, "The pathogenesis of cancer metastasis: The 'seed and soil' hypothesis revisited," *Nature Reviews Cancer*, vol. 3, no. 6, pp. 453–458, 2003.
- [3] S. Halldorsson, E. Lucumi, R. Gómez-Sjöberg, and R. M. Fleming, "Advantages and challenges of microfluidic cell culture in polydimethylsiloxane devices," *Biosensors and Bioelectronics*, vol. 63, pp. 218–231, 2015.
- [4] S. J. Morrison, P. M. White, C. Zock, and D. J. Anderson, "Prospective identification, isolation by flow cytometry, and in vivo self-renewal of multipotent mammalian neural crest stem cells," *Cell*, vol. 96, no. 5, pp. 737–749, 1999.
- [5] D. Pappas and K. Wang, "Cellular separations: A review of new challenges in analytical chemistry," *analytica chimica acta*, vol. 601, no. 1, pp. 26–35, 2007.
- [6] P. Paterlini-Brechot and N. L. Benali, "Circulating tumor cells (ctc) detection: Clinical impact and future directions," *Cancer letters*, vol. 253, no. 2, pp. 180–204, 2007.
- [7] E. D. Pratt, C. Huang, B. G. Hawkins, J. P. Gleghorn, and B. J. Kirby, "Rare cell capture in microfluidic devices," *Chemical engineering science*, vol. 66, no. 7, pp. 1508–1522, 2011.
- [8] J. R. Rettig and A. Folch, "Large-scale single-cell trapping and imaging using microwell arrays," *Analytical chemistry*, vol. 77, no. 17, pp. 5628–5634, 2005.
- [9] S. Riethdorf, H. Fritsche, V. Müller, T. Rau, C. Schindlbeck, B. Rack, W. Janni, C. Coith, K. Beck, F. Jänicke, *et al.*, "Detection of circulating tumor cells in peripheral blood of patients with metastatic breast cancer: A validation study of the cellsearch system," *Clinical cancer research*, vol. 13, no. 3, pp. 920–928, 2007.
- [10] E. K. Sackmann, A. L. Fulton, and D. J. Beebe, "The present and future role of microfluidics in biomedical research," *Nature*, vol. 507, no. 7491, pp. 181–189, 2014.
- [11] S. L. Stott, C.-H. Hsu, D. I. Tsukrov, M. Yu, D. T. Miyamoto, B. A. Waltman, S. M. Rothenberg, A. M. Shah, M. E. Smas, G. K. Korir, *et al.*, "Isolation of circulating tumor cells using a microvortex-generating herringbone-chip," *Proceedings of the National Academy of Sciences*, vol. 107, no. 43, pp. 18 392–18 397, 2010.

- [12] W.-H. Tan and S. Takeuchi, “A trap-and-release integrated microfluidic system for dynamic microarray applications,” *Proceedings of the National Academy of Sciences*, vol. 104, no. 4, pp. 1146–1151, 2007.
- [13] L. R. Volpatti and A. K. Yetisen, “Commercialization of microfluidic devices,” *Trends in biotechnology*, vol. 32, no. 7, pp. 347–350, 2014.
- [14] W. M. Weaver, P. Tseng, A. Kunze, M. Masaeli, A. J. Chung, J. S. Dudani, H. Kittur, R. P. Kulkarni, and D. Di Carlo, “Advances in high-throughput single-cell microtechnologies,” *Current opinion in biotechnology*, vol. 25, pp. 114–123, 2014.
- [15] F. Yesilkoy, R. Ueno, B. Desbiolles, M. Grisi, Y. Sakai, B. Kim, and J. Brugger, “Highly efficient and gentle trapping of single cells in large microfluidic arrays for time-lapse experiments,” *Biomicrofluidics*, vol. 10, no. 1, p. 014 120, 2016.
- [16] M. Yu, S. Stott, M. Toner, S. Maheswaran, and D. A. Haber, “Circulating tumor cells: Approaches to isolation and characterization,” *The Journal of cell biology*, vol. 192, no. 3, pp. 373–382, 2011.